10436 *Inorg. Chem.* **2010**, *49*, 10436–10444
DOI: 10.1021/ic101356n

Inorganic Chemistry
Article

Development of an Icosahedral Quasicrystal and Two Approximants in the Ca−Au−Sn System: Syntheses and Structural Analyses

Qisheng Lin and John D. Corbett*

Department of Chemistry, Iowa State University, Ames, Iowa 50010

Received July 7, 2010

The realm of Tsai-type (YCd_6-type) quasicrystals (QCs) and their approximants (ACs) continues to expand to the east in the periodic table. The heavy tetrel Sn is now one of the major components in the new $Ca_{15.0(5)}Au_{60.0(4)}Sn_{25.0(2)}$ (atom %) icosahedral QC and in the corresponding 1/1 and 2/1 ACs. (The 2/1 AC with Yb is also established.) Single-crystal X-ray diffraction on a 1/1 AC gives the refined formula of $Ca_3Au_{14.36(3)}Sn_{4.38(5)}$ in space group $Im\bar{3}$, a = 15.131(1) Å, whereas a representative 2/1 AC gives $Ca_{13}Au_{47.2(1)}Sn_{28.1(1)}$, $Pa\bar{3}$ and a = 24.444(1) Å. Both ACs contain five-shell multiply endohedral triacontahedral clusters as the common building blocks, as in the parent structure of YCd_6. The 2/1 AC also contains four Ca_2-dimer-centered prolate rhombohedra (PRs) in the unit cell. The long-range order between triacontahedra and PRs in the 2/1 AC is the same as those in Bergman-type 2/1 ACs. A TB-LMTO-ASA calculation on an ideal 1/1 AC model reveals a shallow pseudogap in the total densities-of-states data around the Fermi energy, as expected. The depth of the pseudogap is considerably enhanced through interactions between the Ca 3d states and s and p states of Au and Sn.

Introduction

Quasicrystals (QC), which are characteristic intermetallic compounds, are a class of crystals that exhibit incompatible rotational symmetries (5-, 8-, 12-fold etc.) and thus defy the periodicity rules of classic crystallography.[1] The special arrangement of atoms in QCs in turn produces certain characteristic physical properties (e.g., low surface energy, friction coefficient, and thermal conductivity and high tensile strength) that keep QCs in the forefront in material sciences and technologies.[2] The aperiodicity of QCs can be in one, two, or three dimensions, the last showing the noncrystallographic icosahedral symmetry $m\bar{3}\bar{5}$.[1] So far, three types of icosahedral QCs (*i*-QCs) are known: Bergman, Mackay, and Tsai types. These are well-differentiated by the short-range orders (SROs) of clusters in the respective approximant crystals (ACs) $Mg_{32}(Al,Zn)_{49}$,[3] α-(Al, Mn,Si),[4] and YCd_6.[5] The ACs are conventional crystalline materials, but they are assumed to possess structural units and chemical compositions similar to those in corresponding QCs. The lattice parameter ($a_{q/p}$) of a cubic AC of order q/p has a fixed numeric relationship to the lattice constant (a_6) of the corresponding *i*-QC indexed with six integers via Elser's method:[6] $a_{q/p} = 2a_6(p + q\tau)/(2 + \tau)^{1/2}$, in which p and q are two consecutive Fibonacci numbers.[1,7] Accordingly, an *i*-QC can be considered a cubic crystal with an infinitely large unit cell, and the higher the order of an AC, the closer its structure approaches that of *i*-QC. In this sense, ACs can play even more important roles than *i*-QC because the former can be structurally characterized and their composition−structure−property relationships can be conveniently established, whereas straightforward structural solutions and electronic structure calculations for *i*-QCs remain impractical so far.

In general, electrons in QCs and ACs tend to be delocalized and to lead to bonding interactions that are more covalent in nature,[8] meaning that the transfer of electrons from electropositive to electronegative components is incomplete. Therefore, they can also be grouped into the family of electron-poorer polar intermetallics,[9,10] but their structures cannot be rationalized via the well-known octet rule, Zintl−Klemm,[11,12] Wade−Mingos,[13,14] or other concepts developed for those intermetallics containing closed-shell polyhedral clusters. Rather, they tend to follow the Hume−Rothery

*To whom all correspondence should be addressed. E-mail: jcorbett@iastate.edu.

(1) Janot, C. *Quasicrystals: A Primer*, 2nd ed.; Oxford University Press: Oxford, U.K., 1994.
(2) Dubois, J. M. *Useful Quasicrystals*; World Scientific: River Edge, NJ, 2005.
(3) Bergman, G.; Waugh, J. L. T.; Pauling, L. *Acta Crystallogr.* **1957**, *10*, 254.
(4) Mackay, A. L. *Acta Crystallogr.* **1962**, *15*, 916.
(5) Larson, A. C.; Cromer, D. T. *Acta Crystallogr.* **1971**, *27B*, 1875.
(6) Elser, V. *Phys. Rev. B* **1985**, *32*, 4892.
(7) Goldman, A. I.; Kelton, K. F. *Rev. Mod. Phys.* **1993**, *65*, 213.
(8) Hashimoto, K.; Yamada, Y.; Yamauchi, T.; Tanaka, T.; Matsuda, T.; Mizutani, U. *Mater. Sci. Eng., A* **2003**, *181*−*182*, 785.
(9) Corbett, J. D. *Inorg. Chem.* **2010**, *49*, 13.
(10) Miller, G. J.; Lee, C.-S.; Choe, W. In *Inorganic Chemistry Highlights*; Meyer, G., Naumann, D., Wesemann, L., Eds.; Wiley-VCH: Weinheim, Germany, 2002; pp 21−53.
(11) Schäfer, H.; Eisenmann, W.; Müller, W. *Angew. Chem., Intl. Ed. Engl.* **1973**, *12*, 694.
(12) von Schnering, H. G. *Nova Acta Leopold.* **1985**, *59*, 165.
(13) Mingos, D. M. P. *Acc. Chem. Res.* **1984**, *17*, 311.
(14) Wade, K. *Adv. Inorg. Chem. Radiochem.* **1976**, *18*, 1.

Published on Web 10/12/2010

stabilization mechanism[15] manifested by the coincidence of Fermi surface and Brillouin zone plane in reciprocal space.[16] A Hume−Rothery phase often exhibits a pseudogap in its densities-of-states (DOS) at the Fermi energy (E_F) and shows a relatively small range of electron counts per atom (e/a).[17] For Tsai-type *i*-QCs, e/a values are around 2.0.[18]

After the debut of the binary $YbCd_{5.67}$ *i*-QC,[19] other Tsai-type QCs and their ACs have been extensively studied by scientists from diverse research fields.[18,20−25] ACs of Tsai-type *i*-QCs (or YCd_6-type ACs) to date consist of an alkali-earth or rare-earth metal (e.g., Ca, Sc, Yb) and one or two metals from groups 11−13.[22,26] These elements are neighbors in the periodic table to those in conventional Zintl phases.[22] Therefore, the development of novel YCd_6-type ACs is of particular interest because knowledge of structure and bonding implications within them may in turn improve the understanding of electron-poor polar intermetallics and help to find missing links between Hume−Rothery, polar intermetallics, and Zintl phases.

In recent years, we have continued to develop Tsai-type QC systems containing elements near the Zintl border. For example, we have reported the syntheses, structures, and aspects of the bonding of a series of ACs and evidence of *i*-QCs in the Sc−Cu−Zn,[27,28] Sc−Mg−Cu−Ga,[29] Sc−Mg−Zn,[30,31] Ca−Au−In,[32] and Ca−Au−Ga[33] ternary systems, with the last four following our pseudogap tuning route.[29] Recently, we found that the YCd_6-type phases also exist in the M−Au−Ge (M = Ca and Yb) systems,[34] which, for the first time, included the metalloid Ge in YCd_6-type compounds.

However, no *i*-QC phase and corresponding 2/1 AC were found in the M−Au−Ge systems under our routine conditions,[34] in contrast to those with the triels In and Ga.[32,33] The reason appears to lie mainly in size factors. The structure of $Ca_3(Au,Ge)_{19}$, which exhibits the same structural motif as the prototypic YCd_6, is only stable at low Ge percentages (< 22.0 atom %). Above this, the structure changes into $Ca_{3.25}(Au,Ge)_{18}$ with Ge % > 23.8 atom % in which the innermost shell is a single atom, in contrast to the disordered tetrahedron in $Ca_3(Au,Ge)_{19}$ and YCd_6. Therefore, parallel reactions in the Ca−Au−Sn system were run with the hope that the larger sized Sn would not only stabilize the YCd_6-type AC structures but also yield an *i*-QC phase.

In this work, we found both 1/1 and 2/1 ACs and the *i*-QC in the Ca−Au−Sn system, as expected,[35] whereas Morita and Tsai[36] reported only the existence of a 2/1 AC phase with a nominal composition $Ca_{15}Au_{65}Sn_{20}$. A structure from powder X-ray data of $Ce_3Au_{13.8}Sn_{3.4}$, a 1/1 AC relative, has also been reported.[37] Group 14 metalloids Si and Ge have been found to form Mackay-type *i*-QCs such as $Al_{60}Cr_{20}Si_{20}$ and $Al_{60}Cr_{20}Ge_{20}$,[38] but no p-block metals to the right of the triels (Al, Ga, In) have yielded any QC before. The availability of Ca−Au−Sn *i*-QC pushes the boundary of *i*-QC closer to the classic Zintl phase elements.

Experimental Section

Synthesis. The starting materials were high purity elements: Ca chunks (99.99%, Aldrich-APL, surface cleaned with surgical blade), Au particles (99.99%, Ames Laboratory), and Sn pieces (99.9%, Alfa-Aesar). They were weighed in a N_2-filled glovebox (H_2O < 0.1 ppm vol) to give a total of ∼400 mg for each reaction. Mixtures were put into 9-mm-diameter Ta containers that were weld-sealed under Ar and in turn enclosed in an evacuated SiO_2 jacket (< 10^{-5} Torr) to avoid air oxidation at elevated temperatures.

As before,[34] a series of reactions with $CaAu_{6-x}Sn_x$ (x = 3.5, 4.0, 4.5, with e/a = 2.08, 2.33, 2.58, respectively) was run first to check the availability of a YCd_6-type quasicrystal and approximant phases. These samples were heated at 850 °C for 24 h, slowly cooled to 500 °C (2 °C/h), annealed there for three weeks, and then quenched in water. Phase analyses revealed that all of these were dominated (> 70% yield) by a cubic phase ($a \approx$ 24.45 Å, space group $Pa\bar{3}$) that was isostructural with the early reported $Ca_{13}Au_{57.1}Ga_{23.4}$ 2/1 AC,[33] as confirmed by both powder and single-crystal X-ray diffraction. This suggested a good opportunity to tune both quasicrystal and a lower order 1/1 AC in the Ca−Au−Sn system. Therefore, reactions over wider composition ranges were run under the same or similar conditions (some reactions were instead annealed at 400 °C). In contrast to the fact that two distinctive YCd_6 derivatives exist in the Ca−Au−Ge system,[34] $Ca_3Au_{14.48(7)}Sn_{4.25(8)}$ is the only 1/1 AC present in the composition range around Ca/Au/Sn = (10−14):(66−70):20. Its phase width also appears to be very small, as indicated by the small variation of the a lattice parameters, ∼6σ, see Table 1. In comparison, the 2/1 AC lattice parameters vary from 24.426(1) to 24.457(1) Å, indicating a larger phase width.

To check the availability of the *i*-QC phase, a reaction with nominal composition $Ca_{14.5}Au_{60.1}Sn_{24.5}$ that produced a high yield of the 2/1 AC phase after annealing at 500 °C (Table 1) was directly quenched from 850 °C in water. Both powder and single-crystal X-ray diffraction (Figure 1) confirmed that the product was dominated by an *i*-QC phase. EDX measurements revealed that the proportions of the *i*-QC phase are $Ca_{15.0(5)}Au_{60.0(4)}Sn_{25.0(2)}$ (e/a = 1.90).

Four Yb−Au−Sn reactions parallel to 2, 3, 4, and 12 in Table 1 were also loaded, including that for the 1/1 AC in the Ca system. These all gave high yields of the 2/1 AC phase according to powder

(15) Hume-Rothery, W. *J. Inst. Met.* **1926**, *35*, 295.
(16) Jones, H. *Proc. Phys. Soc.* **1937**, *49*, 250.
(17) Mizutani, U. In *The Science of Complex Alloy Phases*; Massalski, T. B., Turchi, P. E. A., Eds.; TMS (The Minerals, Metals & Materials Society): Warrendale, PA, 2005; pp 1−42.
(18) Tsai, A. P. In *The Science of Complex Alloy Phases*; Massalski, T. B., Turchi, P. E. A., Eds.; TMS (The Minerals, Metals & Materials Society): Warrendale, PA, 2005; p 201.
(19) Tsai, A. P.; Guo, J. Q.; Abe, E.; Takakura, H.; Sato, T. J. *Nature* **2000**, *408*, 537.
(20) Fornasini, M. L.; Manfrinetti, P.; Mazzone, D.; Dhar, S. K. *Z. Naturforsch.* **2008**, *63b*, 237.
(21) Ishimasa, T. In *The Science of Complex Alloy Phases*; Massalski, T. T., Turchi, P. E. A., Eds.; TMS (The Mineral, Metals & Materials Society): Warrendale, PA, 2005; p 231.
(22) Lin, Q.; Corbett, J. D. *Struct. Bonding* (*Berlin*) **2009**, *133*, 1.
(23) Pay Gómez, C.; Lidin, S. *Phys. Rev. B* **2003**, *68*, 024203.
(24) Piao, S.; Gomez, C. P.; Lidin, S. *Z. Naturforsch.* **2006**, *61b*, 644.
(25) Takakura, H.; Pay Gómez, C.; Yamamoto, Y.; De Boissieu, M.; Tsai, A. P. *Nat. Mater.* **2007**, *6*, 58.
(26) Villars, P.; Calvert, L. D. *Pearson's Handbook of Crystallographic Data for Intermetallic Phases*, 2nd ed.; American Society of Metals: Materials Park, OH, 1991; Vol. *1*.
(27) Lin, Q.; Corbett, J. D. *Philos. Mag. Lett.* **2003**, *83*, 755.
(28) Lin, Q.; Corbett, J. D. *Inorg. Chem.* **2004**, *43*, 1912.
(29) Lin, Q.; Corbett, J. D. *J. Am. Chem. Soc.* **2005**, *127*, 12786.
(30) Lin, Q.; Corbett, J. D. *J. Am. Chem. Soc.* **2006**, *128*, 13268.
(31) Lin, Q.; Corbett, J. D. *Philos. Mag.* **2006**, *86*, 607.
(32) Lin, Q.; Corbett, J. D. *J. Am. Chem. Soc.* **2007**, *129*, 6789.
(33) Lin, Q.; Corbett, J. D. *Inorg. Chem.* **2008**, *47*, 7651.
(34) Lin, Q.; Corbett, J. D. *Inorg. Chem.* **2010**, *49*, 4570.
(35) Corbett, J. D.; Lin, Q. In Exploring for new approximants and quasicrystals according to chemical experience and intuition. *10th International Conference on Quasicrystals*, Zurich, Switzerland, July 6 −11, 2008; ETH: Zurich, Switzerland, 2008.
(36) Morita, Y.; Tsai, A. P. *Jpn. J. Appl. Phys.* **2008**, *47*, 7975.
(37) Kenzari, S.; Demange, V.; Boulet, P.; de Weerd, M. C.; Ledieu, J.; Dubois, J. M.; Fournée, V. *J. Phys.: Condens. Matter* **2008**, *20*, 095218.
(38) Inoue, A.; Kimura, H. M.; Masumoto, T.; Tsai, A. P.; Bizen, Y. *J. Mater. Sci. Lett.* **1987**, *6*, 771.

Table 1. Some Reaction Compositions, Products, and Refined Lattice Constants for 1/1 and 2/1 ACs and *i*-QC Phases in the Ca−Au−Sn System

code	Ca/Au/Sn (atom %)	conditions[b]	products and estimated yields[c]	lattice constants (Å)[a]		
				powder data	single crystal data	refined crystals
1	14.3/42.9/42.9	850/500	75% CaAuSn + 5% AuSn + 20% $AuSn_2$			
2	14.3/50.0/35.7	850/500	80% 2/1 AC + 10% CaAuSn + 10% AuSn	24.457(1)		
3	15.0/52.5/32.5	850/400	>95% 2/1 AC	24.440(1)	24.444(1)	**2**
4	14.3/57.1/28.6	850/500	95% 2/1 AC + 5% *P*6/*m*	24.437(1)		
5	14.5/60.1/25.4	850/500	92% 2/1 AC + 8% *P*6/*m*	24.429(1)		
6	14.5/60.1/25.4	850/quench	90% *i*-QC + U_1	5.493(5)		
7	14.3/64.3/21.4	850/500	90% 2/1 AC + 10% *P*6/*m*	24.426(1)		
8	14.3/71.4/14.3	850/500	U_2			
9	20.0/60.0/20.0	850/500	70% *P*6/*m*[c] + 30% 2/1 AC			
10	20.0/55.0/25.0	850/400	80% *P*6/*m* + 10% CaAuSn + U_3			
11	13.0/67/0/20.0	850/500	90% 1/1 AC + 10% *P*6/*m*	15.1248(6)	15.131(1)	**1**
12	10.0/70.0/20.0	850/400	70% 1/1 AC + 25% 2/1 AC + 5% AuSn	15.1211(6)		
13	10.0/65.0/25.0	850/400	90% 2/1 AC + 10% AuSn	24.457(1)		
14	10.0/55.0/35.0	850/400	80% 2/1 AC + 20% AuSn	24.435(1)		

[a] Powder lattice parameters of 1/1 and 2/1 ACs and *i*-QC were refined from the five strong peaks within $2\theta = 30-65°$. Note the parameter for *i*-QC was obtained using Elser's method; its relationship with lattice parameters of ACs is given in the text. [b] Only the heating and annealing temperatures are listed here, for others, see the text. [c] The percentages were estimated according to observed peak intensities in powder patterns. *P*6/*m* is a new hexagonal phase, $Gd_{14}Ag_{51}$-type. U_x ($x = 1-3$) are three unidentified phases.

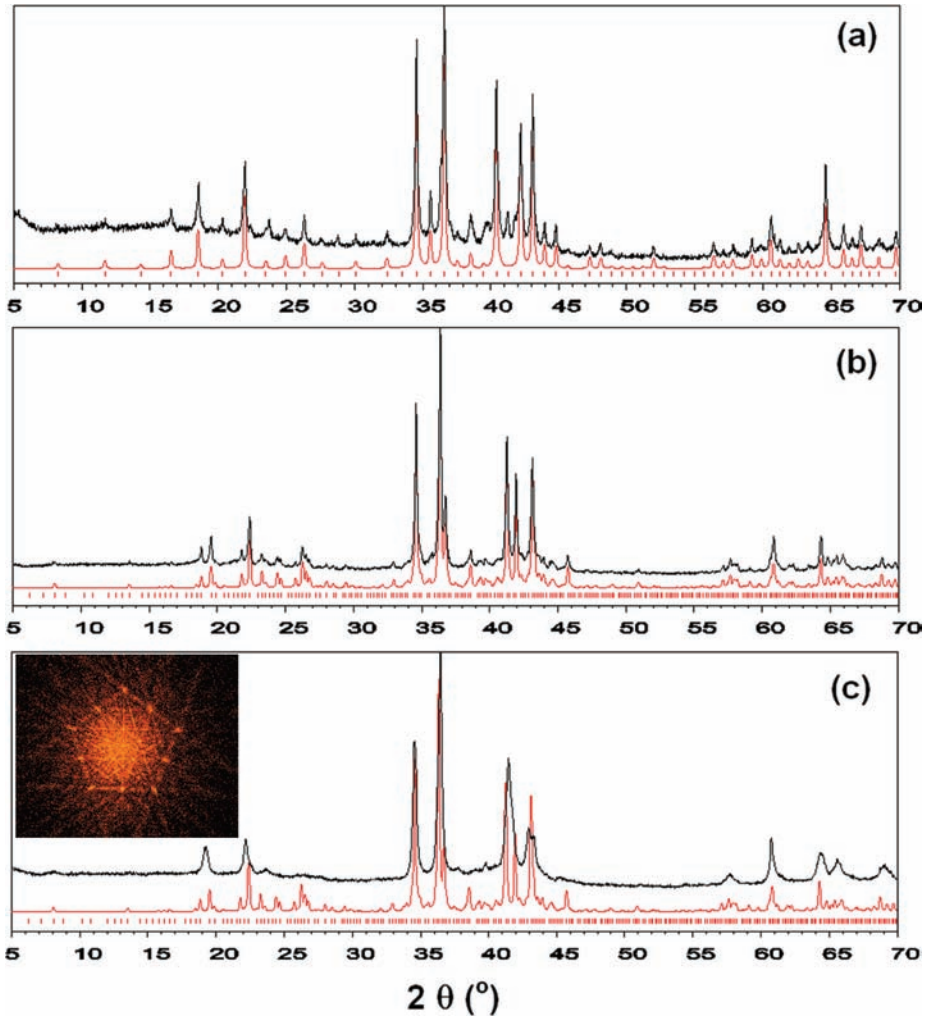

Figure 1. Experimental (black) and calculated (red) X-ray powder patterns from single-crystal data of (a) 1/1 and (b) 2/1 ACs and (c) *i*-QC. Note that the simulated 2/1 AC pattern is compared with experimental data for *i*-QC in c. The inset in c shows the 5-fold symmetry from single quasicrystal X-ray diffraction data.

X-ray diffraction results. This suggests that the Yb−Au−Sn 2/1 AC also has a large phase field. No further attempts were made to gain the corresponding 1/1 AC and *i*-QC though.

All reactions yield brittle products with metallic lusters. The products visually appear to be inert to moisture and air at room temperature for two years. Single crystals were directly selected

from crushed samples, and other portions were ground into fine powders for phase analyses.

Phase Analyses. These were made on the basis of powder diffraction data collected on a Huber 670 Guinier powder camera equipped with an area detector and Cu Ka_1 radiation (λ = 1.540598 Å). The detection limit of a second phase with this instrument and system is conservatively estimated to be about 5 vol % in equivalent scattering power. Phase identification was done with the aid of PowderCell,[39] and lattice parameters of 1/1 and 2/1 ACs and *i*-QC were refined by using strong peaks within 20−70° in 2θ with the aid of the program UnitCell.[40]

Powder patterns of products containing high yields of the 1/1 and 2/1 ACs and *i*-QC phases in the Ca−Au−Sn systems are presented in Figure 1, together with calculated patterns using respective single crystal data (below) or the observation of 5-fold symmetry in an *i*-QC single crystal (inset). This figure gives some general knowledge about the similarities and differences in powder patterns among the 1/1 and 2/1 ACs and *i*-QC. As can be seen, the powder pattern of the higher order 2/1 AC is closer to that of corresponding *i*-QC than the low order AC.

SEM-EDX. Elemental compositions were determined via semiquantitative energy-dispersive X-ray spectroscopy (EDX) on a JEOL 59101v scanning electron microscope (SEM). Samples were mounted in epoxy, carefully polished, and then sputter-coated with a thin layer of carbon prior to loading into the SEM chamber. Accelerating voltages were 20 keV. Samples were first scanned by means of backscattered electrons, through which different phases were recorded by regions with different darknesses. Elemental proportions for selected single-phase areas were then measured. At least four readings were made on each sample, and the averages were compared with the refined compositions from X-ray diffraction data.

Single Crystal Diffraction of *i*-QC. Single grain *i*-QC can have regular polyhedral shapes (e.g., triacontahedron,[41] dodecahedron,[42,43] etc.) under certain reaction conditions. However, no regular morphology was found for our *i*-QC, although a high yield was achieved (Figure 1c). Hence, the single icosahedral quasicrystal selected for single-crystal X-ray diffraction had no visible difference from the conventional crystals under the microscope.

However, the diffraction patterns of conventional crystals and quasicrystals are quite different in the reciprocal space. For traditional crystals, no 5-fold symmetry can be found in any direction, and indexing of the diffraction peaks is conventional. For a quasicrystal, one will frequently fail to index diffraction peaks or sometimes encounter very large cell constants, say, larger than 100 Å. However, patterns that clearly exhibit 5-fold symmetry after suitable rotations in reciprocal space are readily found with the help of X-RED,[44] as shown in the inset in Figure 1c. Here, each sharp "line" corresponds to a collection of parallel, equally spaced layers in reciprocal space. Actually, all icosahedral symmetry elements can be found through suitable rotations in the three-dimensional reciprocal space. However, structure determination of the present *i*-QC is beyond this work because it requires manpower, six-dimensional crystallographic knowledge, and special programs to handle the diffraction data.[25]

Structure Determinations. Single crystals of a Ca−Au−Sn 1/1 (**1**) and a 2/1 AC (**2**) were mounted on a Bruker APEX CCD single crystal diffractometer equipped with graphite-monochromatized Mo Kα (λ = 0.71069 Å) radiation. Intensity data were collected at room temperature with an ω scan method over 2θ = ~3−57° and with exposures of 30 s per frame. Both sets of reflections were consistent with cubic $m\bar{3}$ symmetry and could be indexed by body-centered and primitive lattices, respectively. The R_{int} values for observed reflections [$I > 3\,\sigma(I)$] for **1** and **2** were 9.03% and 14.71%, respectively. Customarily, such data sets are dominated by low intensity reflections. Data integration, Lorentz polarization, and other corrections were made with the SAINT subprogram included in the SMART software package.[45] Numerical absorption corrections were performed with the aid of X-Shape.[46]

Table 2. Some Data Collection and Refinement Parameters for Crystals **1** and **2**

crystal	**1**	**2**
formula	$Ca_3Au_{14.48(7)}Sn_{4.25(8)}$	$Ca_{13}Au_{47.2(1)}Sn_{28.1(1)}$
e/*a*	1.72	2.10
fw	3477.04	13153.05
space group/*Z*	$Im\bar{3}$/8	$Pa\bar{3}$/8
latt. param (Å)	15.130(1)	24.444(1)
vol (Å^3)/d_{cal} (g/cm^3)	3464.2(4)/13.33	14605.5(10)/11.96
abs. coeff. (mm^{-1})	128.96	104.69
refln coll./R_{int}	15204/0.0903	124012/0.1471
data/restr./params	767/0/57	5779/0/310
GOF on F^2	1.18	1.12
R1/wR2 [$I > 3\sigma(I)$]	0.0326/0.0576	0.0592/0.0857
res. peaks (e Å^{-3})	2.92/−4.06	4.11/−2.49

Direct methods were used to set up the initial structural models, and full-matrix least-squares refinements on F^2 and Fourier syntheses were carried out with the aid of the SHELXTL program.[47] Atomic types were assigned according to isotropic displacement parameters and site occupancies. Refinements of both structures yielded reasonable atomic parameters except that isotropic displacement parameters of Sn7 in **1** and Sn57 in **2** were about 5−7 times larger than the averages of others. Examinations of Fourier maps revealed that electron densities of both sites had complex and irregular shapes (Figure S1, Supporting Information). (Why these atoms have irregular electron densities is not known, but it is possibly related to imperfect absorption corrections.) The observations suggest that the conventional anisotropic displacement parameters, which correspond to second-order anharmonic parameters, are not good enough to describe a 3D ellipsoid. Rather, additional anharmonic tensors would give better descriptions of their thermal displacements. Therefore, both structures were refined with third and fourth anharmonic tensors for the pathological atoms with the JANA2006 program.[48] (Note that all of the third anharmonic components for crystal **1** refined to zero, as required by the specific electron density shape, Figure S1.) The refined anharmonic tensors for both atoms are given in Table S1 in the Supporting Information. The refinements were consistently improved by this step, as indicated by the R_w values (5.72% verse 5.81% for **1**, 8.57% verse 9.17% for **2**). Later on, independent structural determinations by means of a charge−flipping algorithm applied by Superflip[47] in JANA2006 were tried, and these gave the same results, suggesting correct structural models had been obtained. The refined compositions of crystals **1**, $Ca_3Au_{14.39(7)}Sn_{4.35(8)}$, and **2**, $Ca_{13}Au_{47.2(1)}Sn_{28.1(1)}$, agree well with corresponding EDX data, $Ca_3Au_{14.7(1)}Sn_{4.6(2)}$ and $Ca_{13}Au_{48.2(1)}Sn_{29.0(1)}$, respectively.

The crystallographic data and structure refinement parameters for both crystals are given in Table 2. The refined positional and isotropic−equivalent displacement parameters for both crystals are

(39) Roisnel, T.; Rodríguez-Carvajal, J. In WinPLOTR: a Windows tool for powder diffraction patterns analysis, Materials Science Forum. *Proceedings of the Seventh European Powder Diffraction Conference* (*EPDIC 7*); Delhez, R.; Mittenmeijer, E. J., Eds.; Scitec Publications, Ltd: Chennai, India, 2000; pp 118−123.
(40) Holland, T. J. B.; Redfer, S. A. T. *Miner. Mag.* **1997**, *61*, 65.
(41) Kaneko, Y.; Ishimasa, T. *Jpn. J. Appl. Phys.* **2002**, *41*, L1268.
(42) Fisher, I. R.; Islam, Z.; Panchula, A. F.; Cheon, K. O.; Kramer, M. J.; Canfield, P. C.; Goldman, A. I. *Philos. Mag.* **1998**, *77*, 1601.
(43) Canfield, P. C.; Caudle, M. L.; Ho, C.-S.; Kreyssig, A.; Nandi, S.; Kim, M. G.; Lin, X.; Kracher, A.; Dennis, K. W.; McCallum, R. W.; Goldman, A. I. *Phys. Rev. B* **2010**, *81*, 020201(R).
(44) *X-AREA*, v 2.10; STOE & Cie Gmbh: Darmstadt, Germany, 2003.
(45) *SMART*; Bruker AXS, Inc.: Madison, WI, 1996.
(46) *X-Shape*, version 1.03; Stoe & Cie: Darmstadt, Germany, 1998.
(47) *SHELXTL*; Bruker AXS, Inc: Madison, WI., 2000.
(48) Petříček, V.; Dušek, M.; Palatinus, L. *JANA*; Institute of Physics: Praha, Czech Republic, 2006.

Table 3. Atomic Coordinates and Isotropic Equivalent Displacement Parameters for 1/1 AC, $Ca_3Au_{14.39(7)}Sn_{4.35(8)}$ (**1**), and 2/1 AC, $Ca_{13}Au_{47.2(1)}Sn_{28.1(1)}$ (**2**)

atom	Wyck.	occ.	*x*	*y*	*z*	U_{eq} (Å^2)
			1/1 AC			
Au1	48*h*	1	0.1083(1)	0.3424(1)	0.2011 (1)	0.027(1)
Au2	24*g*	1	0	0.4052(1)	0.3483(1)	0.017(1)
Au31	16*f*	0.825(3)	0.1541(1)	0.1541(1)	0.1541(1)	0.033(1)
Au32	16*f*	0.175(3)	0.0950(3)	0.0950(3)	0.0950(3)	0.033(1)
Au4	12*d*	1	0.4084(1)	0	0	0.021(1)
Au/Sn5	24*g*	0.52/0.48(1)	0	0.2490(1)	0.0900(1)	0.021(1)
Sn6	12*e*	1	0.1893(1)	0	1/2	0.017(1)
Sn7	8*c*	0.75(2)	1/4	1/4	1/4	0.099(4)[b]
Au/Sn8	24*g*	0.11/0.22(1)	0	0.0645(3)	0.0857(3)	0.021(1)
Ca9	24*g*	1	0	0.1884(3)	0.3040(3)	0.017(1)
			2/1 AC			
Sn11	24*d*	0.333[a]	0.1925(5)	0.6517(7)	−0.0932(6)	0.023(4)
Sn12	24*d*	0.333[a]	0.3208(10)	0.3475(8)	0.2888(7)	0.052(7)
Sn13	24*d*	0.333[a]	0.1183(10)	0.8456(1)	0.2853(8)	0.059(8)
Sn14	24*d*	0.333[a]	0.1183(9)	0.6544(11)	−0.0930(9)	0.064(8)
Au/Sn21	24*d*	0.51/0.49(3)	0.1543(2)	0.7138(1)	0.0006(1)	0.023(1)
Au/Sn22	24*d*	0.81/0.19(3)	0.1545 (2)	0.9057(1)	0.1912(1)	0.031(1)
Au/Sn23	24*d*	0.84/0.16(3)	0.1539(2)	0.5963(1)	−0.0010(2)	0.036(1)
Au/Sn24	24*d*	0.61/0.49(3)	0.1531(2)	0.7870(1)	0.1917(1)	0.027(1)
Au25	24*d*	1	0.2525(2)	0.4406(2)	0.2520(2)	0.042(1)
Au26	24*d*	1	0.0584(1)	0.7490(1)	−0.0587(1)	0.029(1)
Au27	8*c*	1	0.0566(8)	0.0566(8)	0.0566(8)	0.028(1)
Au28	8*c*	1	0.2559(2)	0.2559(2)	0.2559(2)	0.060(1)
Ca31	24*d*	1	0.0361(7)	0.6545(9)	0.0334(7)	0.031(4)[c]
Ca32	24*d*	1	0.2728(5)	0.6539(7)	0.0345(6)	0.017(3)[c]
Ca33	24*d*	1	0.1539(7)	0.6580(6)	0.2321(5)	0.022(3)[c]
Ca34	24*d*	1	0.0386(4)	0.8485(6)	0.1577(6)	0.013(2)[c]
Ca35	8*c*	1	0.040 (1)	0.040(1)	0.040(1)	0.05(1)[c]
Au/Sn40	24*d*	0.55/0.45(3)	−0.0301(2)	0.5538(2)	0.0809(2)	0.023(1)
Au/Sn41	24*d*	0.82/0.18(3)	0.0702(2)	0.7182(1)	0.1444(2)	0.028(1)
Au/Sn42	24*d*	0.60/0.40(2)	0.1545(2)	0.8505(2)	0.0917(1)	0.026(1)
Au/Sn43	24*d*	0.50/0.50(4)	0.0723(2)	0.7825(2)	0.0489(2)	0.030(2)
Au/Sn44	24*d*	0.72/0.28(3)	0.2370(2)	0.7181(2)	0.1461(2)	0.032(2)
Au/Sn45	24*d*	0.60/0.40(3)	0.2176(2)	0.5478 (2)	0.2634(2)	0.033(2)
Au/Sn46	24*d*	0.35/0.65(3)	0.1537(2)	0.6509(2)	0.0989(1)	0.031(1)
Au/Sn47	24*d*	0.45/0.55(3)	0.3581(2)	0.5742(2)	−0.0263(2)	0.038(2)
Au/Sn48	24*d*	0.32/0.68(4)	0.2309(3)	0.5290(2)	0.0520(2)	0.043(2)
Au/Sn49	24*d*	0.39/0.61(3)	0.2331(2)	0.9728(2)	0.1423(3)	0.051(2)
Au51	24*d*	1	0.2472(2)	0.5975(2)	0.1569(2)	0.024(1)
Au52	24*d*	1	0.0584(1)	0.5974(1)	0.1536(2)	0.029(1)
Au53	24*d*	1	0.3434(2)	0.5578(1)	0.0954(1)	0.034 (1)
Au54	24*d*	1	0.0943 (2)	0.5353 (1)	0.2531 (2)	0.032(1)
Au55	24*d*	1	0.0578 (2)	0.9040 (2)	0.0365 (2)	0.049(2)
Sn56	8*c*	1	0.1562(2)	0.1562(2)	0.1562(2)	0.021(1)
Sn57	24*d*	1	0.0394(6)	0.5452(6)	0.3467(8)	0.117(5)[b]
Sn58	24*d*	1	−0.0357(2)	0.6567(3)	0.1545(3)	0.035(2)

[a] Fixed occupancy. [b] Refined with 3rd and 4th anharmonic tensors, as listed in Table S1 (Supporting Information). [c] Isotropic displacement parameters.

listed in Table 3. For direct comparisons, atoms in crystal **1** are sorted according to those for earlier reported Ca−Au−Ge 1/1 AC,[34] whereas those in **2** are sorted according to the sequence of endohedral shells. Detailed crystallographic data are available in the CIF outputs (Supporting Information).

Electronic Structure Calculations. The calculation for **1** was performed by means of the self-consistent, tight-binding, linear-muffin-tin-orbital (LMTO) method in the local density (LDA) and atomic sphere (ASA) approximations, within the framework of the DFT method.[49−52] ASA radii were scaled automatically at the limit of 18% maximum overlap between neighboring atomic spheres, and three interstitial spheres were introduced accordingly. The average ASA radii for Ca, Au, and Sn were about 3.98, 2.83, and 2.82 Å, respectively. Reciprocal space integrations were carried out by means of the tetrahedron method. The basis sets were 3d/4s/(4p) for Ca, 6s/6p/5d/(5f) for Au, and 5s/5p/(5d) for Sn, with orbitals in parentheses down-folded.[53] Scalar relativistic effects were automatically included in the calculations. The band structure was sampled for 24 × 24 × 24 *k* points in the irreducible wedge of the Brillouin zone.

Results and Discussion

Partial Phase Diagram. Until now, orthorhombic CaAuSn (*Pnma*)[54] was the only ternary compound with a known structure in the Ca−Au−Sn system. According

(49) Tank, R.; Jepsen, O.; Burkhardt, A.; Andersen, O. K. *TB-LMTO-ASA Program*, Vers. 4.7; Max-Planck-Institut für Festkörperforschung: Stuttgart, Germany, 1994.
(50) Shriver, H. L. *The LMTO Method*; Springer-Verlag: Berlin, Germany, 1984.
(51) Jepsen, O.; Snob, M. *Linearized Band Structure Methods in Electronic Band-Structure and its Applications, Springer Lecture Notes*; Springer Verlag: Berlin, Germany, 1987.
(52) Anderson, O. K.; Jepsen, O. *Phys. Rev. Lett.* **1984**, *53*, 2571.
(53) Lambrecht, W. R. L.; Andersen, O. K. *Phys. Rev. B* **1986**, *34*, 2439.
(54) Kubsmann, D.; Hoffmann, R.-D.; Pöttgen, R. *Z. Anorg. Allg. Chem.* **1998**, *624*, 1727.

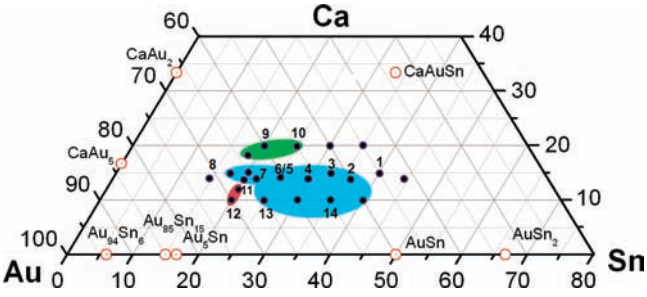

Figure 2. Approximate phase fields of 1/1 (red) and 2/1 ACs (blue) and a new hexagonal phase (green, see text)) in the Ca−Au−Sn system at 400−500 °C. Note that the phase fields are represented by random ovals that include just our limited reactions; real widths may vary. Black dots represent reactions run; the numbers are as in Table 1.

to our experimental results (Table 2), at least three more Au-rich ternary phases exist in the 400−500 °C section. Their compositions are $Ca_3Au_{14.39(7)}Sn_{4.35(8)}$ (1/1 AC, e/a = 1.72), $Ca_{13}Au_{36.0(1)}Sn_{39.9(1)}$ (2/1, e/a = 2.10), and $Ca_7Au_{23.7(1)}Sn_{2.4(1)}$ according to single crystal refinements. Of these, the last is a new polar intermetallic with $P6/m$ symmetry.[55] As noted above, the *i*-QC phase $Ca_{15.0(5)}Au_{60.0(4)}Sn_{25.0(2)}$ (atom %; e/a = 1.90) also exists, but it is only available by quenching.

Figure 1 shows the electron-poor corner of the Ca−Au−Sn phase triangle. As can be seen, the formation of the 1/1 AC phase is limited to a very narrow phase field (shaded in red), around ca. $Ca_{10-13}Au_{67-70}Sn_{20}$. In contrast, the 2/1 AC phase forms in a much wider phase range (blue), ca. $Ca_{10-20}Au_{50-65}Sn_{20-40}$ (Table 1). This could explain why Morita and Tsai only observed the supposed 2/1 AC phase in their experiments.[36] A comparison between Ca−Au−Ge and Ca−Au−Sn phase triangles reveals three remarkable differences: first, the 1/1 AC phase region in Ca−Au−Ge is split into two discrete subregions at ∼500 °C, one for $Ca_3(Au,Ge)_{19}$ and the other for $Ca_{3.25}(Au,Ge)_{18}$.[34] However, the latter does not occur in the Ca−Au−Sn system in the same composition and temperature ranges. Second, reactions in the composition range Ca/Au/Ge = (10−20):(50−65):(20−40) always yield the 1/1 AC phase after annealing at 400−500 °C.[34] In contrast, the 2/1 AC dominates the products of parallel Ca−Au−Sn reactions. Third, only the 1/1 AC relatives are known in the Ca−Au−Ge system, whereas not only 1/1 and 2/1 ACs but also the *i*-QC phase occurs in the Ca−Au−Sn system under our experimental conditions.

Crystal Structures. The 1/1 AC $Ca_3Au_{14.39(7)}Sn_{4.35(8)}$ (**1**) crystallizes in space group $Im\bar{3}$, with a = 15.131(1) Å, and the 2/1 AC $Ca_{13}Au_{47.2(1)}Sn_{28.1(1)}$ (**2**) in $Pa\bar{3}$, with a = 24.444(1) Å (Figure 2). The lattice parameter of the 2/1 AC is about 1.615 times larger than that of the 1/1, close to the golden mean (τ = 1.618). According to equation $a_{q/p} = 2a_6(p + q\tau)/(2 + \tau)^{1/2}$, the calculated quasicrystal lattice constant (a_6) with the 1/1 AC as a reference is about 5.497(1) Å, agreeing well with the measured quasilattice constant, 5.493(5) Å, Table 1. These facts support the conclusion that **1** and **2** are truly ACs of the *i*-QC $Ca_{15.0(5)}Au_{60.0(4)}Sn_{25.0(2)}$ (EDX data). As before,[5,23,28,30,32−34,56] AC structures are best described in terms of their short-range orders (SROs) and the long-range orders (LROs) of these structural units. Here, SROs include the geometries and atomic decorations of the five-shell endohedral clusters ending with the triacontahedra, whereas LROs refer to the arrangement of triacontahedra-based unit cells in 3D space.

1/1 AC. The multiply endohedral shells, or SRO motif, in the 1/1 AC are shown in Figure 3a−e. The innermost shell (a) is generated by Au/Sn8 atoms with a refined occupancy of 33(1)%. Therefore, there are actually 12 × 0.33 = 4 atoms in this shell, and according to the local symmetry, this shell is commonly considered a 3-fold-disordered tetrahedron.[5,19] Interestingly, this innermost shell in the reported structure of $Ce_3Au_{13.8}Sn_{3.4}$[37] is missing, the same as in the erroneously reported structure of Sc_3Zn_{17}.[57] The second shell (b) is a dodecahedron defined by 12 Au/Sn5 and 8 Au3 atoms, with the latter located on proper 3-fold axes. The average of surface interatomic separations is about 2.80 Å, comparable to the 2.76 Å sum of Pauling's single bond distances of Au and Sn.[58] The third shell, the only cation location, is defined by 20 Ca atoms with icosahedral geometry. The surface Ca9−Ca9 separations are about 5.70 Å, meaning that they have no significant direct bonding with each other. The electropositive Ca atoms play important roles in defining structural type. As shown in Figure S2 (Supporting Information), each Ca not only caps a pentagonal face of the second shell but also centers a pentagonal face in the fourth shell (d) and caps a pentagonal face of the outmost shell (e). All 16 Ca−Au and Ca−Au/Sn interatomic separations fall in the range of 3.20−3.36 Å, suggesting strong bonding interactions for all of them. The fourth shell is a 30-atom icosidodecahedron (d) defined by 24 Au1 and 6 Au4 atoms, with Au4 occupying vertices in axial directions. The outermost triacontahedral shell consists of 32 vertices and 60 edges. The decoration of this shell is noteworthy: of the 32 ideal vertices, the eight with real 3-fold symmetry are empty, as found in Ca−Au−Ge 1/1 ACs as well, whereas the others are unexceptionally occupied by Sn6 atoms. Thus, the triacontahedron is actually a defect polyhedron.[56] On the other hand, Au atoms occupy the 60 edges of the triacontahedron.

Similar to that in $Ca_3(Au,Ge)_{19}$,[34] the Wyckoff 8*c* sites (0.25, 0.25, 0.25) in the present 1/1 AC are partially occupied (75%) by Sn7. This leads to the deviation of the actual composition from 1:6. Each Sn7 is enclosed in a cube[56] defined by six Au1 and two Au3 atoms, as also shown Figure 3d. In each cube, the two Au3 atoms come from dodecahedral shells centered at the cell origin and body center, three of the six Au1 atoms from the icosidodecahedral shell, and the other three Au1 atoms from the triacontahedral shells. However, it is more convenient to consider Sn7 as an interstitial atom sandwiched between the icosidodecahedral and triacontahedral shells, as in Ga, In, and other parallel compounds.[28,32,33]

The foregoing 5-shell endohedral clusters are arranged in body-center-cubic packing, Figure 3f. Accordingly, each triacontahedral cluster has (8 + 6) like neighbors. The eight nearest neighbors are positioned in 3-fold directions, and each interpenetrates the central triacontahedral cluster with a shared oblate rhombohedron (OR),

(55) Lin, Q.; Corbett, J. D. Unpublished results.
(56) Pay Gómez, C.; Lidin, S. *Angew. Chem., Int. Ed.* **2001**, *40*, 4037.
(57) Andrusyak, R. I.; Kotur, B. Y.; Zavodnik, V. E. *Sov. Phys. Crystallogr.* **1989**, *34*, 600.
(58) Pauling, L. *The Nature of the Chemical Bond*, 3rd ed.; Cornell University Press: Ithaca, NY, 1960; p 403.

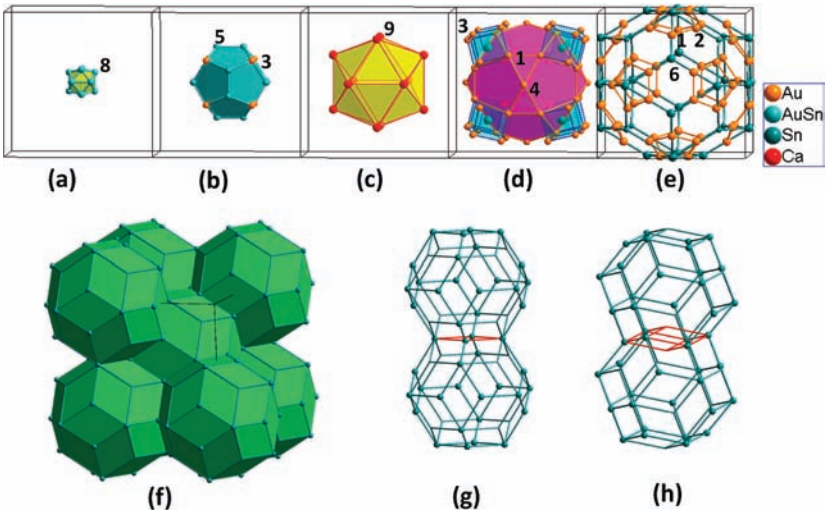

Figure 3. The building block of 1/1 AC, $Ca_3Au_{14.39(7)}Sn_{4.35(8)}$ (**1**), contains, from the center out, (a) a disorder tetrahedron, (b) a dodecahedron, (c) an icosahedron, (d) an icosidodecahedron, and (e) a triacontahedron. For clarity, clusters on the corners of the unit cell are not shown in a−e. The interstitial Sn7 in cubes (blue) are shown in (d). Numbers marks atoms listed in Table 3. These triacontahedral clusters are arranged in body-center-cubic packing (bcc) at the unit cell level, as shown in (f). Note that one cluster at the corner is omitted for clarity in (f). The bcc packing of triacontahedra results in two types of shared linkages between them, i.e., (g) a rhombic face in axial directions or (h) an oblate rhombohedron in body diagonal directions, as emphasized by red lines. The representative color schemes for atoms in a−e are the same for later figures.

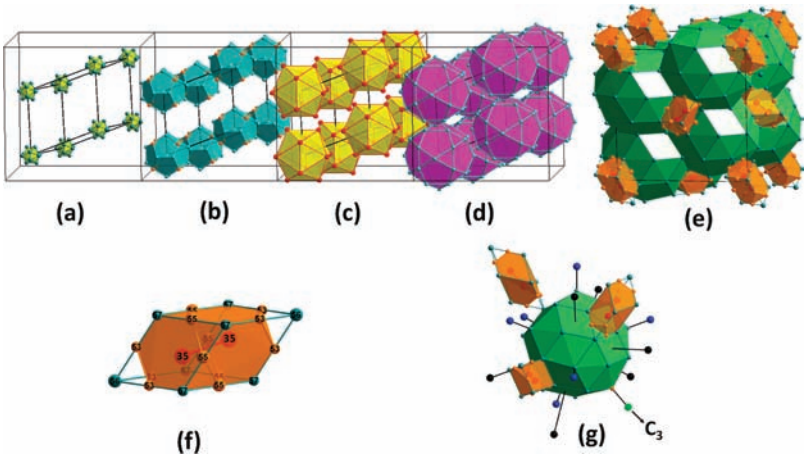

Figure 4. The multiply endohedral clusters in 2/1 AC, $Ca_{13}Au_{47.2(1)}Sn_{28.1(1)}$, from the center out: (a) a disordered tetrahedron, (b) a dodecahedron, (c) an icosahedron, (d) an icosidodecahedron, and (e) a triacontahedron. These triacontahedral clusters are arranged in primitive cubic packing, leaving unfilled spaces in a shape of (f) prolate rhombohedra (PRs), in which the Ca−Ca dimer is centered along the 3-fold direction. Each PR consists of a double Friauf polyhedron (or two face-shared truncated tetrahedra, orange). The linkage between neighboring triacontahedra and PRs is shown in (g). For clarity, only the central triacontahedron is shown as a polyhedron, whereas those sharing rhombic faces with the central polyhedron on pseudo-2-fold axes are represented only by solid black spheres, those that share oblate rhombohedra (ORs) on pseudo-3-fold axes by blue, and that on real 3-fold axes by a green sphere.

as shown in Figure 3(g). The six second-nearest neighbors are located on 2-fold axes, each sharing a face with the central cluster, Figure 3(h). Such a LRO arrangement is in clear contrast to that in the 2/1 AC (below).

2/1 AC. This structure also contains giant triacontahedral clusters as building blocks. The SRO within the triacontahedron is shown in Figure 4a−f. Compared to that in the 1/1 AC, most differences are resulted from the lower symmetry for the 2/1, which means more variables are necessary to define cluster geometries and more atomic species, to decorate the former. For example, the dodecahedral (b) and icosahedral shells (c) appear to have no major differences from the corresponding shells in the 1/1, but the actual symmetry is 3 rather than $m\bar{3}$ in 1/1. Thus, the vertices of the icosidodecahedral shell (d) are all occupied by Au/Sn mixtures, not the pure Au in the 1/1. It should be noted that the outermost triacontahedral shells in the 2/1 AC are fully defined by different types of atoms, i.e., Sn (56×4, 57×9, 58×12), Au (27), and their mixtures Au/Sn (21×3, 24×3), in contrast to the defect version in 1/1 (Table 3). A plot of all vertex and decoration atoms is given in Figure S3a (Supporting Information). A detailed comparison of shell contents in these 1/1 and 2/1 ACs is given in Table 4, together with a comparison with those in Ca−Au−In[32] and Ca−Cd[23,56] analogues.

Compared with 2/1 ACs in other systems,[30,32,33,56,59] the new scenario in the present 2/1 AC is that the innermost shell has a configuration of a 3-fold disordered tetrahedron, the same as 1/1 AC. Different configurations for this shell have been reported in other 2/1 ACs, e.g., a regular ordered tetrahedron in the structures of $Sc_{11.2}Mg_{2.5}Zn_{73.6}$ and

(59) Pay Gómez, C.; Morita, Y.; Yamamoto, A.; Tsai, A. P. *J. Phys.: Conf. Ser.* **2009**, *165*, 012045.

Table 4. Comparison of Shell Contents within Triacontahedra for 1/1 and 2/1 ACs of Ca−Au−T (T = Sn, In, Cd) Systems

	Ca−Au−Sn		Ca−Au−In		Ca−Cd	
	$Ca_3Au_{14.4}Sn_{4.4}$ (1/1)	$Ca_{13}Au_{47.2}Sn_{28.1}$ (2/1)	$Ca_3Au_{12.4}In_{6.1}$ (1/1)	$Ca_{12.6}Au_{37.0}In_{39.6}$ (2/1)	Ca_3Cd_{18} (1/1)	$Ca_{13}Cd_{75.9}$ (2/1)
e/*a*	1.74	2.10	1.73	2.01	2.0	2.0
tetrahedron	$Au_{1.2}Sn_{2.8}$	Sn_4	In_4	$In_{3.5}$	Cd_4	$Cd_{3.9}$
dodecahedron	$Au_{14.2}Sn_{5.8}$	$Au_{16.3}Sn_{3.7}$	$Au_{15.3}In_{4.7}$	$Au_{10.2}In_{9.3}$	Cd_{20}	Cd_{20}
icosahedron	Ca_{12}	Ca_{12}	Ca_{12}	Ca_{12}	Ca_{12}	Ca_{12}
icosidodecahedron[a]	$Au_{30}(Sn_6)$	$Au_{17.4}Sn_{12.6}$	$Au_{20.7}In_{9.3}(In_{3.8})$	$Au_{11}In_{19}$ ($In_{1.6}$)	Cd_{30}	Cd_{30}
triacontahedron[b]	Sn_{24} [Au_{60}]	$Au_{3.4}Sn_{29.6}$ [$Au_{51.4}Sn_{8.6}$]	In_{24} [$Au_{54}In_6$]	$In_{29.6}$ [$Au_{48}In_{12}$]	Cd_{24} [Cd_{60}]	Cd_{32} [$Cd_{60.2}$]
reference	this work	this work	32	32	23	56

[a] Contents in parentheses are fractional atoms located between shells. [b] Contents in square brackets are decorations at or near edge centers of the triacontahedron.

$Ca_{12.6}Au_{37.0}In_{39.6}$;[30,32] a monotruncated tetrahedron in $Ca_{13}Au_{57.1}Ga_{23.4}$;[33] and irregular polyhedra in $Ca_{13}Cd_{76}$ and $Yb_{13}Cd_{76}$.[56] This is ascribed to the nearly ideal geometry for the dodecahedral shell in the present 2/1 AC, see Figure 4(b). Prior to this study, the dodecahedra shells in all other 2/1 AC analogues were found to be heavily distorted as a result of "being pushed" by split sites or neighboring interstitials.

Figure 4e shows the unit cell in terms of triacontahedral clusters. As can be seen, primitive cubic packing of triacontahedral clusters cannot completely fill the space, leaving $(8 \times 1/8 + 6 \times 1/2) = 4$ prolate rhombohedra (PR) in the unit cell. As matter of fact, each PR holds a double Friauf polyhedron (or two face-shared truncated tetrahedra) that is centered by Ca35−Ca35 dimers (d_{Ca-Ca} = 3.36 Å), Figure 4(f).

The LRO of triacontahedra and PRs in the 2/1 is very complex. To simplify, a triacontahedron is taken as the subject and only its linkages to other triacontahedra and PRs are described here. Each triacontahedron has (6 + 1 + 6) like neighbors plus four PRs arranged with C_3 symmetry, as shown in Figure 4(g). Among these, 13 like neighbors, the six represented by blue spheres lie on pseudo-3-fold axes, and the one in green on a real 3-fold axis; each of these neighbors shares an oblate rhombohedron (OR) with the central triacontahedron, Figure S3 (b) (Supporting Information). On the other hand, the remaining six neighbors in black locate on pseudo-2-fold axes, and each shares a rhombic face with the central triacontahedron, Figure S3 (c). This LRO is in great contrast to that of 1/1 AC, in which each triacontahedron has (8 + 6) like neighbors. However, the same LRO exists in all other 2/1 ACs, including the Bergman-type 2/1 ACs.[22]

Electronic Structure. The smaller and less complex structure of the 1/1 AC was modified as follows for a calculation. First, positions 1 to 5 in the sequence in Table 3 were assumed to be fully occupied by Au, with the minor split site (Au32) being omitted, and atoms in sequence 6−8 were assigned to Sn. Then, the 3-fold disordered tetrahedron was circumvented, as before,[32,33,60] by reduction of the symmetry to subspace group *I*23 and by a slight reorientation to match the symmetry requirements. As a result, a model with a formula of "$Ca_3Au_{12.5}Sn_{6.5}$" was constructed, but it should be noted that its *e*/*a* value (2.02) is much larger than that in the real example (1.74).

Figure 5 shows the densities-of-states (DOS) for this hypothetical "$Ca_3Au_{12.5}Sn_{6.5}$". The total DOS pattern is very spiky, characteristic of QCs and ACs, and it shows of

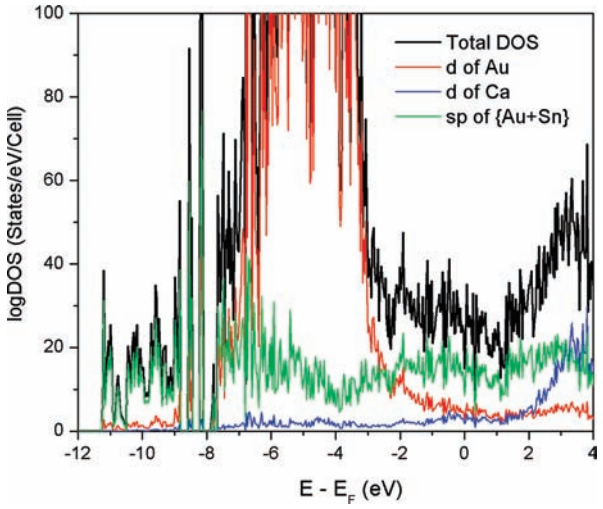

Figure 5. The densities of states (DOS) of a hypothetical 1/1 AC model $Ca_3Au_{12.5}Sn_{6.5}$.

a pseudogap ~0.7−1.1 eV above the Fermi energy (E_F).[61] The DOS spectrum also shows characteristic properties of polar intermetallics compounds,[9] in which the s and p states of Au and Sn spread over the whole energy range, but the Au 5d states mainly populate in the energy range of −8.0 to −3.0 eV, with a small number of states extending to E_F and above. In contrast, Ca d states are mainly located above E_F, with a few states extending to energies below E_F, that is, mixing in the bonding.

As noted above, Ca plays important roles in structural stabilization because of its large size and direct bonding to numerous Au and Sn atoms. In terms of electronic structure, the importance of Ca is also apparent. Judging from the partial DOS curves, Ca d states (red) evidently enhance the depth of the pseudogap through interactions between Ca d and Au/Sn s and p states. Therefore, both size and d states evidently make Ca unique in forming ACs and *i*-QC (relative to Mg, which has no d states, and to Sr, which is evidently too large). This is also the reason why $Na_{30}Au_{39}Sn_{12}$[62] prefers the Bergman- rather than Tsai-type structure.

Summary of YCd_6-Type Structures. Although the 1/1 AC, $Ca_3Au_{14.36(3)}Sn_{4.38(5)}$, is slightly off the 1:6 stoichiometry because of Sn7 inclusion in interstitial sites

(60) Ishii, Y.; Fujiwara, T. *Phys. Rev. Lett.* **2001**, *87*, 206408.

(61) Fujiwara, T.; de Laissaidiere, G. T.; Yamamoto, S. *Mater. Sci. Eng., A* **1994**, *179*−*180*, 118.

(62) Doering, W.; Seelentag, W.; Buchholz, W.; Schuster, H. U. *Z. Naturforsch.* **1979**, *34b*, 1715.

(above), it is still convenient to consider it as a derivative of the YCd_6-type structure, as before.[34] To date, the majority of the YCd_6 family are Zn- and Cd-based phases, including 18 binary RCd_6 phases (R = Ca or rare-earth metals),[26] two binary Zn phases ($ScZn_6$[28] and $YbZn_{\sim 6}$[20]), and two Zn-based ternary phases $Sc(T,Zn)_6$ (T = Mg, Cu).[28,30] (The last group could also include T = Mn, Fe, Co, Ni, Ag, Au, Pt, Pd, etc. transition metals,[63,64] but no structural data for this group have been reported.) The remaining YCd_6-like examples come mainly from ternary triel (Al, Ga, In) phases, i.e., $Yb(Zn,Al)_{\sim 6}$,[20] $Sc(Cu,Ga)_{\sim 6}$,[65] $Ca(Au,Ga)_{\sim 6}$,[33] $Ca(Au,In)_{\sim 6}$,[32] and $Eu(Ag,In)_{\sim 6.3}$.[59] Recently, the YCd_6 family was found to expand to group 14, i.e., $M_3(Au,Ge)_{19}$ and $M_{3.25}(Au,Ge)_{18}$.[34] The present $Ca_3(Au,Sn)_{\sim 19}$ compound is yet another example.

Overall, these examples demonstrate that the realm of the YCd_6 family has expanded from group 12 (Zn and Cd) to group 13 (Al, Ga, In) and group 14 (Ge, Sn) in terms of the electronegative components. The e/a range for this type of phases is $\sim$1.73−2.15,[28,34] this large range occurring because not only the electronegative part but also the electropositive part can be tuned. In these systems, size and electronic factors play crucial roles in phase stabilization as manifested by the fact that the increase of valence electrons, say, from Cd (two valence electrons) to In (three) to Sn (four), is balanced by adjustments of the alloying proportions in four of the five shells (Table 4). It is reasonable to expect that more YCd_6-type phases will be found through chemical tuning. However, those that will also contain QC neighbors will be a smaller set because of poorer chances to achieve suitable compromises among the narrow e/a range, size factors ("fit"), bonding, and electronic factors. Particularly, the gain of QCs containing group 15 and 16 elements (As, Sb, Bi; Se, Te) seems to be increasingly unlikely inasmuch as the bonding for these elements is usually more directional, as often guided by the octet rule, and the s states become increasingly core-like.

Conclusions

In summary, we have succeeded in the high yield syntheses of Ca−Au−Sn 1/1 and 2/1 ACs and *i*-QC through fairly routine high-temperature reactions and tuning. Formerly, the most electron-rich elements in Mackay-type *i*-QC systems have been Si and Ge metalloids, i.e., $Al_{60}Cr_{20}Si_{20}$ and $Al_{60}Cr_{20}Ge_{20}$ *i*-QCs,[38] whereas in Bergman- and Tsai-type *i*-QC systems, they have been only Al, Ga, and In. This discovery gives the first example of a Sn-rich *i*-QC, $Ca_{15.0(5)}Au_{60.0(4)}Sn_{25.0(2)}$ (atom %), demonstrating that the realm of Tsai-type *i*-QCs extends further east[66] in the periodic table. This pushes the boundary of elements possible in Hume−Rothery phases closer to that of Zintl phases and polar intermetallics without increasing e/a. Great opportunities in science may exist here.

The different products achieved between Ca−Au−Ge and Ca−Au−Sn systems are notable. The present system contains both 1/1 and 2/1 ACs and *i*-QC, with a large phase field for 2/1 and small for 1/1 AC. On the contrary, the system with the smaller Ge contains only two well-differentiated 1/1 relatives. In addition, a structural novelty exists in the present 2/1 AC, with a 3-fold disordered tetrahedron in the innermost shell, the same as 1/1. In contrast, all earlier reported 2/1 ACs have very different configurations.

Acknowledgment. This research was supported by the U.S. National Science Foundation, Solid State Chemistry, via grant DMR−0444657 and −0853732. All of the work was performed in the facilities of the Ames Laboratory, U.S. Department of Energy.

Supporting Information Available: Table S1, Figures S1−S3, and CIF data are available free of charge via the Internet at http://pubs.acs.org.

(63) Kashimoto, S.; Maezawa, R.; Kasano, Y.; Mitani, T.; Ishimasa, T. *Jpn. J. Appl. Phys.* **2003**, *42*, L1268.
(64) Maezawa, R.; Kashimoto, S.; Ishimasa, T. *Philo. Mag.* **2008**, *88*, 13.
(65) Markiv, V. Y.; Belyavina, N. N.; Gavrilenko, I. S. *Izvest. Akad. Nauk SSSR, Met.* **1984**, *5*, 227.
(66) Corbett, J. D. Exploratory synthesis: The fascinating and diverse chemistry of polar intermetallic phases. 235th ACS National Meeting, New Orleans, LA, 2008.